



HAL
open science

Deterministic processes drive the microbial assembly during the recovery of an anaerobic digester after a severe ammonia shock

Laëtitia Cardona, Laurent Mazéas, Olivier Chapleur

► To cite this version:

Laëtitia Cardona, Laurent Mazéas, Olivier Chapleur. Deterministic processes drive the microbial assembly during the recovery of an anaerobic digester after a severe ammonia shock. *Bioresource Technology*, 2022, 347, pp.126432. 10.1016/j.biortech.2021.126432 . hal-03871174

HAL Id: hal-03871174

<https://hal.inrae.fr/hal-03871174v1>

Submitted on 25 Sep 2023

HAL is a multi-disciplinary open access archive for the deposit and dissemination of scientific research documents, whether they are published or not. The documents may come from teaching and research institutions in France or abroad, or from public or private research centers.

L'archive ouverte pluridisciplinaire **HAL**, est destinée au dépôt et à la diffusion de documents scientifiques de niveau recherche, publiés ou non, émanant des établissements d'enseignement et de recherche français ou étrangers, des laboratoires publics ou privés.

Title

Deterministic processes drive the microbial assembly during the recovery of an anaerobic digester after a severe ammonia shock

Authors

Laëtitia Cardona^{a1}, Laurent Mazéas^a, Olivier Chapleur^{a*}

^a*Université Paris-Saclay, INRAE, PRocédés biOtechnologiques au Service de l'Environnement, 92761, Antony, France*

**Corresponding author*

laetitia.cardona@epfl.ch

laurent.mazeas@inrae.fr

olivier.chapleur@inrae.fr

Abstract

Anaerobic digestion allows to produce sustainable energy but the microbial community involved in this process is highly sensitive to perturbations. In this study, a longitudinal experiment was performed in two sets of triplicate bioreactors to evaluate the influence of ammonia addition on AD microbiome and its recovery. Zeolite was added in three reactors to mitigate the inhibition. Microbial dynamics were monitored with 16S rRNA sequencing at 15 time points. Dominant methanogenic pathways were determined with gas isotopic signature analysis. Zeolite addition did not enable to reduce ammonia inhibition or improve the process under the conditions tested. In all the bioreactors, ammonia inhibition sharply decreased the methane production but the process could restart thanks to the increase of hydrogenotrophic archaea and syntrophic bacteria. Interestingly, similar behaviour was observed in the six reactors. Neutral modelling and null model were used and showed that a deterministic process governed the recovery of AD microbiome after failure.

Keywords

Pulse disturbance – anaerobic digestion – phylogenetic beta diversity – neutral model

**Corresponding author: olivier.chapleur@inrae.fr*

¹EPFL ENAC IIE LBE – Station 6 – 1015 Lausanne, Switzerland

Introduction

Anaerobic digestion is a microbe-driven bioprocess producing renewable energy from organic waste. Since its first use, the bioprocess has known many technical and operational developments. Recently, and thanks to the democratisation of powerful biomolecular technologies, the microbiome driving the bioprocess has progressively left the black box to a grey zone. For example, the existence of a core microbiome coexisting with specific microbial niches has been recognized (Treu et al., 2016). These niches and more generally the variability of the microbial community are correlated to different operational parameters. Better understanding the microbial response to operational modification, more specifically in case of inhibition, is essential for an appropriate management of the process, to obtain a more stable and performant biogas production.

One of the most influent factors in the bioprocess is the concentration of ammonia. While ammonia is a necessary element for microbial growth, protein-rich substrates such as food waste are usually reported to cause process failure due to the release of ammonia nitrogen during their degradation (Akindele and Sartaj, 2018). Two forms of ammonia exist: the ionised NH_4^+ form and free ammonia NH_3 . The total ammonia nitrogen (TAN) is the sum of these two forms of ammonia. A wide range of concentrations half inhibiting methane production has been described in the literature, ranging from 0.05 to 1.4 $\text{gNH}_3\text{-N/L}$ and from 1.7 to 19 gTAN/L for respectively NH_3 and TAN. Chen et al. (2008) attributed this dispersion to several parameters such as pH, temperature but also to the acclimation of the microbial community (Chen et al., 2008). The succession of microbial and molecular events behind the ammonia inhibition is still unclear but different assumptions have been made, as reviewed by (Jiang et al., 2019). On an operational point of view, the ammonia inhibition is usually followed by a decrease of the pH due to an accumulation of the volatile fatty acids in the bioreactors. This accumulation can be linked to the response of the microbial community facing ammonia. Indeed, volatile fatty acids (VFA) degraders, such as *Syntrophobacter* or acetoclastic methanogen *Methanosaeta*, seem to be the most sensitive population of community facing an elevation of ammonia concentration (Bonk et al., 2018). After a certain latency, a predominance of slow-growing hydrogenotrophic archaea, less sensitive to the ammonia, generally allows the production of the methane. The presence of syntrophic acetate oxidising bacteria is

often reported in association with this archaea. They enable to oxidise the acetate into H₂ and CO₂ consumed by the hydrogenotrophic archaea (Wang et al., 2015). This pathway is called the syntrophic acetate oxidation (SAO).

One way to mitigate the inhibition is the addition of zeolite. Zeolite is a natural rock formed from ashes and volcanoes rocks. In anaerobic system, zeolite has been shown to limit the inhibitory effect of molecules like ammonia (Poirier et al., 2017). In a previous study, it was observed the preservation of the syntrophic communities, mostly syntrophic propionate degraders, associated to hydrogenotrophic methanogens, thanks to the use of zeolite in presence of ammonia (Cardona et al., 2020). Mode of action of the zeolite is not clear, but its role of growth support for the microorganisms is supported by previous studies. For example Fernandez et al. (2007) have demonstrated the development of Methanosaeta and Methanosarcinaceae on the zeolite using fluorescence in situ hybridization (Fernández et al., 2007).

On a more general perspective, two main mechanisms guide the microbial community structuration, stochasticity and determinism. It is generally admitted that deterministic mechanisms are driven by the environmental pressure and species traits while the stochastic mechanisms are driven by random birth, death and dispersal (Chase and Myers, 2011). AD microbiome assembly is probably triggered by this ecological niche theory but until recently it was poorly described. Some authors, such as Peces et al (2018) or Vanwonterghem et al (2014) estimated that deterministic processes shape the microbial community assembly during long-term experiment using dissimilarity analyses. More recently, Lin et al al (2019) studied the influence of the temperature on the AD microbial structuration using null model analyses. Modelling-based methods, coming from ecological studies, were also developed to estimate the relative contribution of the different processes to microbial community assembly (Sloan et al., 2006; Stegen et al., 2012; Zhou et al., 2014). If they are used more often in different microbial ecosystems, there are still seldom used to describe the microbial assembly processes involved in AD systems and even less in case of strong inhibition and recovery periods. In the present study, null model based analysis were used in complement to multivariate analysis in order to fill this gap.

The present study aims at providing a description of AD microbiome dynamics during a complete process failure due to an abrupt addition of ammonia followed by the

recovery of the process. More precisely, the ability of the different members of the microbial community to overcome or not this inhibition was depicted. For that purpose, a long-term experiment was carried out in replicated lab-scale bioreactors and the microbial community was subjected to a high and rapid ammonia concentration increase. Zeolite was added into three bioreactors in order to evaluate the influence of the mineral support on the microbial structuration and bioreactors recovery after ammonia inhibition. The temporal dynamics of the microbiome was evaluated using 16S rRNA amplicon sequencing. The main methanogenic pathway was determined using the measurement of the isotopic composition of the biogas. The relative contribution of the stochastic mechanisms into the microbial community assembly was assessed using Sloan's Neutral Community Model and null models (Sloan et al., 2006; Yuan et al., 2019).

Material and methods

Feedstock preparation

Food biowaste was used to feed bioreactors. This biowaste came from an industrial food deconditioning plant and had different origins such as schools, markets, expired products, products for quality testing. It was stored at -20°C. Each week, enough quantity was thawed and grounded prior to use to prepare the feedstock. The inoculum came from a mesophilic full scale anaerobic bioreactor treating primary sludge from a wastewater treatment plant (Valenton, France).

Experimental set-up

Six semi-continuous stirred tank reactors (CSTR, Bioprocess Control) were operated in mesophilic condition during 231 days. The parameters used to operate this experiment are described below: working volume of 5 L (7 L total), constant agitation of 90 rpm, constant organic loading rate (OLR) of 0.5 gCOD/L/Day and hydraulic retention time (HRT) of 25 days. The feeding was prepared once a week and stored at 4°C with the following composition: 87 g of biowaste diluted in biochemical methane potential buffer (based on BMP-International Standard ISO 11734 (1995)) to reach a final working volume of 2 L. The buffer composition is as follow: 0.27 g/L K₂HPO₄, 1.12 g/L Na₂HPO₄-12H₂O, 0.08 g/L CaCl₂-2H₂O, 0.1 g/L MgCl₂-4H₂O, 0.02 g/L FeCl₂-4H₂O, Na₂S-9H₂O, 11.76 g/L NaHCO₃. As substrate was biowaste, a

complex mixture of organic residues, we assumed that there was no shortage of trace elements in the bioreactors.

Zeolite was added into three bioreactors, called hereafter Z1, Z2 and Z3, at the beginning of the experiment (15 g/L), while the three other bioreactors were kept as control without zeolite (C1, C2 and C3). During the first 70 days, corresponding to 3 HRT, the bioreactors were operated to reach stable performances (Phase 1). Then, ammonia ((NH₄)₂CO₃) was added abruptly in all the bioreactors to reach a final concentration of NH₄⁺ of 4 gNH₄⁺/L after less than 1 day. This concentration was determined from previous batch experiments (data not shown) to inhibit the methane production. The bioreactors were fed with a feeding containing the same concentration of ammonia (Phase 2). Because the biogas production stopped totally, it was decided to stop the feeding after 14 days. Absence of feeding for 45 days (Phase 3) until the biogas production and the volatile fatty acids consumption restarted. Bioreactors were then fed again with a feeding containing 2 g/L of ammonia to maintain a low concentration inside the bioreactor (Phase 4, 102 days). A schematic representation of the experiment is available on figure 1.

Chemical analyses

The biogas production flow was measured using a μ Flow (Bioprocess Control). The biogas was collected into a Tedlar® bag. The biogas composition was analysed directly from the bioreactor headspace using a micro gas chromatograph (CP4900, Varian).

The methanogenic pathways (acetoclastic methanogenesis or hydrogenotrophic methanogenesis) were determined through the gas isotopic signature analysis. Periodically gas was sampled into a 7-mL vacuumed serum tube for the analysis of $\delta^{13}\text{C}_{\text{CH}_4}$ and $\delta^{13}\text{C}_{\text{CO}_2}$. A Trace Gas Chromatograph Ultra (Thermo Scientific) attached to a Delta V Plus isotope ratio mass spectrometer via a GC combustion III (Thermo Scientific) was used to carry out the analysis. Using an autosampler 100 μL of samples were injected (Triplus AS, Thermo Electron Corporation) into the gas chromatograph (GC) equipped with a Paraplot Q column to separate the CH₄ to the CO₂. The parameters used for this separation were a split mode with a ratio of 20 at 150°C. The sequence for the GC was: 3 min at 35°C, increase of temperature to 180°C and stabilisation of 24 seconds at 180°C. The gas vector flux (helium) was

constant at 1.8 mL/min. The separated CH₄ and CO₂ went through the combustion oven (940°C) to transform the gas into CO₂. The CO₂ was ionised in the mass spectrometer electronic impact source into CO₂⁺ and the different ions were separated according to their mass/charge (m/z) ratio. The isotopes were detected by three different collectors on the trajectories of the isotopomeres with m/z of 44 (12C16O₂), 45 (13C16O₂ and 12C17O16O) and 46 (12C16O18O, 13C16O17O, 12C17O17O). The isotopic ratios 45/44 and 46/45 were calculated and compared to the ones of a reference CO₂ injected at the beginning and at the end of the samples analysis. The δ¹³C expressed in ‰ was then calculated as presented in the following equation:

$$\delta^{13}C = \left[\frac{(R_e - R_s)}{R_s} \right] \cdot 1000$$

Where Re corresponds to the ratio 13C/12C of the sample and Rs corresponds to the ratio 13C/12C of the international standard. As an indicator of the methanogenic pathway, the apparent isotopic factor (α_{app}) was calculated as presented in the following equation (Whiticar et al., 1986).

$$\alpha_{app} = \frac{(\delta^{13}CO_2 + 10^3)}{(\delta^{13}CH_4 + 10^3)}$$

It is usually assumed that if the α_{app} is superior to 1.065 the hydrogenotrophic way is dominant. On the contrary, if the α_{app} is inferior to 1.055 the methanogenesis is dominated by the acetoclastic way (Whiticar et al., 1986).

The total ammonia nitrogen (TAN) concentration was measured using the Nessler's colorimetric method following the French standard (NF T 90-105) in spectroscopic tanks using Hach spectrometer DR2800. The link between Free Ammonia Nitrogen (FAN), Total Ammonia Nitrogen (TAN), pH and temperature (T in Kelvin) can be summarised with the following equation (Anthonisen et al., 1976):

$$FAN = \frac{10^{pH}}{\left(\exp\left(\frac{6344}{T}\right) + 10^{pH} \right)} \times TAN$$

Volatile Fatty Acids (VFA) concentrations were measured using ionic chromatography (ICS 5000+, Thermo Fisher Scientific) equipped with IonPAC ICE-

AS1 column. The mobile phase was composed of heptafluorobutyric acid (0.4 mmol/L) and tetrabutylammonium (5mmol/L). The VFA quantified were acetate, propionate and butyrate.

In order to compare statistically the biogas production during the recovery period, the Gompertz parameters (lag time and production rate) were estimated for each bioreactor and an analysis of variance (ANOVA) was used to determine if there is a significant difference between both parameters between the bioreactors control (C) and with zeolite (Z).

DNA extraction and 16S rRNA amplicon sequencing

The microbial structure was followed all along the experiment. Each bioreactor was sampled 15 times (90 samples in total) to cover the different phases of the experiment. The DNA was extracted using the commercial kit MOBIO (PowerSoil™ DNA Isolation kit) following the manufacturer's instructions. V4-V5 of the 16S rRNA gene was amplified by PCR with fusion primers 515F (5'- Ion A adapter-Barcode-GTGYCAGCMGCCGCGGTA-3') (Wang et al., 2007) and 928R (5'-Ion trP1 adapter-CCCCGYCAATTCMTTTRAGT-3') (Wang and Qian, 2009), which included a barcode and sequencing adapters. The fusion PCR method used fusion primers to attach the Ion A adapter (5'-CCATCTCATCCCTGCGTGTCTCCGACTCAG-3') linked to a barcode, and the Ion truncated P1 (trP1) adapter (5'-CCTCTCTATGGGCAGTCGGTGAT-3') to the amplicons as they were generated during PCR. Between 5000 and 15000 reads per sample were obtained. The raw sequences were deposit on the NCBI database under the project number PRJNA676039. Samples are referred under the accession numbers from SAMN16751950 to SAMN16752039.

FROGS (Find Rapidly OTU with Galaxy Solution), a galaxy/CLI workflow (Escudie et al., 2018), was used to generate an OTU count matrix, taxonomy assignment and phylogenetic tree. The alignment was done using PyNAST and the phylogenetic tree was built using FastTree.

Determination of the microbial assembly processes

The OTUs table was rarefied using the function "rarefy_even_depth" from the phyloseq R package (McMurdie and Holmes, 2013) (726 OTUs).

Processes governing local community structure (in one sample) was determined using the function “ses.mntd” from picante R package (Kembel et al., 2010). This function allows to calculate the Nearest Taxon Index (NTI) by standardising effect size of the Mean Nearest Taxon Distances (MNTD) (Webb et al., 2002). Briefly, MNTD estimates the average phylogenetic distance between each OTU and its closest relative within a sample. NTI quantifies the number of standard deviations that the observed MNTD is from the mean of the null distribution (after 999 randomizations). NTI greater than +2 indicates that coexisting taxa are more closely related than expected by chance, meaning a phylogenetic clustering of OTUs in the sample. In the opposite, NTI less than -2 indicates coexisting taxa are more distantly related than expected by chance, meaning phylogenetic overdispersion in the sample. A mean NTI taken across all samples that is significantly different from zero indicates clustering (NTI>0) or overdispersion (NTI<0) on average (Stegen et al., 2012).

The potential importance of stochastic processes was evaluated using Sloan’s Neutral Community Model (Sloan et al., 2006). This model predicts the relationship between the frequency of each OTU in each of this experimental Phases (Phase 1, 2, 3 or 4), and their abundance in the overall community, meaning in all Phases. A null model analysis was also performed to calculate the deviation of null expectations from actual observations and thereby quantify the contribution of stochastic processes to community assembly as explained in previous studies (Zhou et al., 2014). Briefly, for each time point in a reactor, the number of species was counted and randomly drawn based on the microbial richness at this time point (1000 iterations). The Jaccard’s similarity between each pair of reactors was calculated after each iteration and an average Jaccard’s similarities at each time point was obtained from the 1,000-time drawing. Then the stochasticity contribution was calculated using the following formula:

$$\% \text{ stochasticity} = 1 - \frac{J_{obs,i} - J_{exp,i}}{J_{obs,i}}$$

where $J_{obs,i}$ is the actual Jaccard’s similarity between two reactors at the time point i and $J_{exp,i}$ is the expected Jaccard’s similarity between two reactors at the time point i . The analysis was done based on the description and R script from Yuan et al. (2019).

Multivariate analysis

For multivariate analysis, OTUs that exceeded 1% in terms of relative abundance in at least one sample were selected. From the 728 OTUs, 98 were kept after the filtering (4 OTUs belonging to the archaea domain and 94 OTUs from the bacteria domain). Abundance data were center-log ratio (clr) transformed.

Multivariate data analysis was carried out using the mixOmics R package (Rohart et al., 2017) using a suite of component-based methods to identify groups of microorganisms. Sparse Principal Component Analysis (sPCA, (Shen and Huang, 2008)), an unsupervised approach, was applied to evidence main sources of variation between samples and identify key OTUs. In this study, the main source of variation corresponded to the ammonia concentration and the microbial capacity to overcome the inhibition. The variable selection from sPCA enabled to identify microorganisms characteristic of the different phases, and also to follow their evolution across time, determine their resilience, resistance or development due to shock of ammonia. The abundances of these microbes were represented in a heatmap drawn with mixOmics package.

Results and discussion

In order to understand the effect of an ammonia shock on the anaerobic microbial dynamics and structuration, 4 gTAN/L of ammonia was added to stabilised bioreactors treating biowaste. Methanogenic pathways, chemical performances and microbial population were analysed to determine which microbes were able to high level of ammonia and allowed to bioprocess to recover. The part of the stochasticity and determinism was determined statistically using null model in order to determine the predictability of the microbial inhibition and recovery.

Influence of ammonia shock on bioreactor performances

The figure 2 represents the chemical parameters (TAN, FAN, biogas production, ratio of CH₄ in biogas, α_{app} , acetate, propionate and pH) measured over the course of the experiment. A summary of the mean values for the different parameters is available in the supplementary material.

Stabilisation phase

During the stabilisation phase (first 70 days) all the bioreactors had a similar behaviour. In 3 bioreactors (Z1 to Z3) the presence of zeolite did not influence the bioprocess performances compared to the control bioreactors (C1 to C3). This result is in line with previous studies indicating the absence of effect of zeolite when ammonia is no present in the system (Cardona et al., 2020; Poirier et al., 2017).

A stable production of methane (representing 80% of the biogas) and biogas (around 450 mL/day) was observed during this stabilisation phase. According to the isotopic fractionation measurement, the methane was mainly produced through the acetoclastic pathway (α_{app} inferior to 1.055). During that period, no VFAs (acetate and propionate) accumulation was observed, indicating a good functioning of the bioprocess. An exception can be noticed for the bioreactors Z1 and C3 where a transient accumulation of acetate and propionate was observed, but lower than 200 mgC/L and 150 mgC/L respectively. However, a rapid consumption of these VFAs was observed for both bioreactors. From the start of the experiment to the end of the stabilisation phase, the TAN and NH₃ concentration decreased progressively from 1500 to 250 mgTAN/L and from 200 to 30 mgNH₃/L. This could be explained by an absence of production or a low accumulation of ammonia due to the low OLR used combined to a high dilution rate due to the addition of BMP buffer. The pH increased from 8 to 8.25 and stabilised at this value. The pH of the reactor C3 was different from all the other bioreactors but reached the same value at the end of the stabilisation. As all the parameters where stable during at least one week, the inhibition phase was started.

Inhibition phase

At day 70, ammonia was added into the feeding to reach the final concentration of 4 gTAN/L in few days for all the bioreactors. As a consequence, the performances were highly affected, in a similar way in all the reactors. The biogas production decreased drastically after the ammonia addition indicating an inhibition of the archaeal activity. An increase in the methane percentage was observed just after the perturbation from 80 to 90% followed by a progressive decrease. To the best of authors' knowledge, a sharp increase of the methane after ammonia inhibition has never been reported. A sharp increase in pH was observed after ammonia addition, it is plausible that carbon dioxide in this experiment was trapped in the liquid phase in the form of carbonate,

explaining the increase of methane ratio. This could also explain the sharp decrease of the α_{app} value from 1.05 to 1.03 observed in all the bioreactors. VFA concentrations remained low.

During this period of drastic inhibition, similar trend in the different performance parameters was observed for all the bioreactors except Z3. Indeed, a lower concentration of TAN was observed in Z3 compared to the other bioreactors, respectively 3400 and 4000 mg/L. This lower ammonia level was associated to an earlier and higher acetate and propionate accumulation just after the ammonia addition (89 Ac-mgC/L and 97 Pr-mgC/L for Z3 versus 0 mg/L for the other bioreactors), showing that inhibition was less intense and that some VFA producers were active.

While Z1, Z2 and Z3 bioreactors contained zeolite since the beginning of the experiment, the inhibition appeared to be as drastic in these bioreactors than in the ones without zeolite.

Perturbation phase

As the degradation performances were greatly reduced, and biogas production stopped, the feeding was stopped at day 84 in all the bioreactors in order to enable the microbial activity to recover. The absence of feeding (phase 3) lasted 45 days.

From day 84 to day 105, several changes were observed. Firstly, the methane ratio decreased in parallel to an accumulation of the VFAs leading to a decrease of the pH and consequently a decrease of the NH_3 concentration. Associated to the decrease of the biogas production, these results indicate an inhibition of the methanogenic activity but not of the fermentative activity, confirming the higher sensitivity of the archaea than the fermenters to the ammonia (Zhang et al., 2018).

After day 105, an increase of the methane percentage was associated to acetate consumption and to a modification on the methanogenic pathway (α_{app} higher than 1.065). It means that the methane production was mainly achieved through the hydrogenotrophic pathway and potentially through the syntrophic acetate oxidation. The acetate was probably oxidised by syntrophic acetate oxidisers into H_2 and CO_2 directly consumed by the hydrogenotrophic archaea. The modification of the

methanogenic pathway under ammonia inhibition was already observed in previous studies (Fischer et al., 2019).

All bioreactors behaved similarly except Z3 where α_{app} evolved differently. It reached a value higher than 1.65 before the other bioreactors (from day 84 to 105), but then decreased to reach a value inferior at 1.55 indicating a return of the acetoclastic pathway for the methane production. This pathway modification can be linked to an earlier return of the biogas production than in the other bioreactors. This delay between bioreactors response could be attributed to a difference in the ammonia concentration, slightly lower in Z3 than in the other bioreactors that induced a less important inhibition.

Recovery phase

Finally, the feeding was restored for all the bioreactors as the chemical results indicated a return to a microbial activity efficient enough to produce biogas. Ammonia was still added into the feeding composition at 200 mgTAN/L in order to maintain the presence of ammonia into the bioreactors but at a lower level than during inhibition. A progressive decrease in the ammonia concentration can be observed until day 175 where the concentration stabilised around 1 gTAN/L, corresponding to a FAN concentration inferior to 200 mgNH₃/L. This period lasted more than 100 days and was stopped when chemical parameters reached stable performances.

In parallel to the decrease of the ammonia concentration, the biogas production increased progressively to finally reach at day 200 a rate between 300 to 400 mL/L depending of the bioreactor. For the bioreactor Z3 this rate was reached before than for the other bioreactors, around day 160, probably due to the lowest ammonia inhibition in this bioreactor compared to the others. The methane ratio rapidly reached 85% after the beginning of the recovery phase, while, based on α_{app} , methane was still produced through the hydrogenotrophic pathway. Then, after day 175 when a stable and low concentration of NH₃ was reached, the methane percentage decreased to 75% in parallel with a decrease of α_{app} indicating a modification of the methanogenic pathway from hydrogenotrophic to acetoclastic.

Rapidly after the restart of the feeding, an important accumulation of VFAs was observed, higher than in phase 3, probably explained by the availability of organic

matter for fermenters, while archaea were not yet ready to consume all of it. After day 161, acetate accumulation finally decreased importantly, followed at day 175 by the consumption of the propionate, indicating the return to steady functioning. The delay between the acetate and propionate consumption can be explained by the unfavourable thermodynamic for propionate degradation (Mawson et al., 1991).

Zeolite was already shown to have a positive effect to limit the effect of ammonia inhibition by reducing the lag phase before the production of biogas and/or by increasing the biogas production and/or methane rate (Cardona et al., 2020; Poirier et al., 2017). However, this effect depends on different parameters such as concentration or particle size (Milán et al., 2001; Montalvo et al., 2005) but also implementation of the zeolite in the bioreactor (Wang et al., 2011). In the present experiment the presence of 15 g/L of zeolite in 3 bioreactors (Z1 to Z3) was not sufficient to limit or alleviate faster the ammonia inhibition (around 4 gTAN/L). Indeed, no significant difference was observed between C and Z bioreactors for the lag phase (p-value of 0.233) or for the rate of production (p-value of .322) using ANOVA. Different hypotheses could explain the absence of mitigation effect during this experiment: 1) The zeolite concentration was not sufficient compared to the concentration of ammonia added. Studies tend to indicate that a specific ratio zeolite/substrate needs to be respected for the zeolite to be beneficial for the methane production (Milán et al., 2001). It is possible that in case of inhibition, if this ratio is not respected, the presence of zeolite is not be helpful to mitigate the inhibition. In the same way, this ratio seem to be highly dependent of the biomass, adapted or unadapted to specific inhibitors such as ammonia (Fotidis et al., 2014). The zeolite used in this study was used with success in two previous studies. Cardona et al (2020) and Poirier et al (2017) observed a mitigation of the ammonia inhibition at respectively 2 gTAN/L and 19 gTAN/L with 15 g/L and 10 g/L of zeolite. The difference with the present study is first the inoculum. It is possible that the biomass used in the present study was not adapted enough and that the ratio zeolite/inhibitor was too low to mitigate properly the inhibition. In addition, the bioreactor typology was different between the studies. In the present study CSTR were used instead of batch in previous studies. 2) The presence of the zeolite at the bottom of the bioreactor did allowed a well colonisation of the biomass. Wang et al (2011) demonstrated the higher mitigation capacity of the

zeolite using a fixed-bed bioreactors instead of dispersing the zeolite at the bottom of the bioreactor.

The parallel evolution of all the performances parameters between the bioreactors could indicate deterministic processes occurring in the microbial assembly responsible of the bioreactors production.

Influence of ammonia shock on the microbial community structure

The community structure was followed over time using 16S rRNA gene amplicon sequencing. For each bioreactor, 15 time points were analysed to cover the different phases of the experiment. The relative abundance of the microbial community is represented for bacteria and archaea communities (see supplementary materials).

The archaeal community abundance represent at the maximum 20% of the microbial community abundance in all the experiment. At the beginning of the experiment (Phase 1) the archaeal community was mainly composed of the genera *Methanosarcina* (5%), *Methanoculleus* (5%) and *Methanosaeta* (5%) of except in Z3 where mostly *Methanosarcina* was representative of the archaeal community (5%). In general, under a threshold level of 1000 mgTAN/L of ammonia, the methane is mostly produced from acetoclastic pathway carried out by *Methanosaeta* and *Methanosarcina*. After ammonia addition (Phase 2 – day 70), the abundance of the genus *Methanosaeta* sharply decreased in all bioreactors. This genus was already described to be more sensitive to the presence of inhibitors such as ammonia than other archaea (Ruiz-Sánchez et al., 2019). The abundance of the genus *Methanoculleus* increased in the bioreactors and became dominant. Its abundance fluctuated between the bioreactors and the different phases of the experiment but it remained the major archaea after ammonia addition. The dynamics of the genus *Methanosarcina* also fluctuated across time, and even if they were not dominant, they were always detected in the bioreactors contrary to *Methanosaeta*. The dynamics of these archaea can be related to the evolution of the α app representing the methanogenic pathway modifications. Indeed, at the beginning of the experiment (Phase 1), the presence of *Methanosaeta* and *Methanosarcina* explained the methane production mainly through the acetoclastic pathway. Both these archaea are able to produce methane using acetate as carbon source. After the ammonia addition, no biogas was produced and the restart of its production was mainly due to

hydrogenotrophic archaea, most probably *Methanoculleus*. This indicates that even if hydrogenotrophic archaea are more resistant in presence of ammonia, they need some time to take the lead in the methane production. Moreover, *Methanoculleus* is one of the archaea usually found to be partner of syntrophic bacteria evolved in the SAO. At the end of the experiment, the archaeal community did not return to the initial composition. No *Methanosaeta* could be detected anymore and *Methanoculleus* remained the major archaea over *Methanosarcina*. This could be explained by the presence of 1000 mgTAN/L of ammonia that was maintained in all the bioreactors while only 200 mgTAN/L of ammonia was present at the beginning of the experiment.

The bacterial community also showed modifications in its composition over the different phases. A similar bacterial community could be observed between all the bioreactors. During the stabilisation period (Phase I), the bacterial community was mainly composed of the orders Anaerolineales (40%), Bacteroidales (40%), Cloacimonadales (10%) and Clostridiales (5%). A similar dynamics across the different bioreactors was observed for these microbes. The abundances of the orders members Cloacimonadales and Anaerolineales decreased after the addition of the ammonia to respectively less than 1% and 5%. The abundance of the order Bacteroidales remained relatively stable across time. However, a modification of the most representative OTU of this order was observed after the ammonia addition. Finally, the abundance of the Clostridiales order increased with the addition of ammonia. As evidenced by previous studies, several syntrophic acetate oxidisers or putative SAOB were identified from this order (Mosbæk et al., 2016).

Some microbes were favoured by the presence of the ammonia. Indeed, MAB03 (class of Clostridia), orders Pseudomonadales and Bacillales appeared during the phase 2 (addition of ammonia) and their abundances increased over the different phases. If the abundance of the major OTU from the order Bacillales, genus *Bacillus*, increased in all the bioreactors, its abundance was higher in the bioreactors C2, C3, Z1 and Z2 than in C1 and Z3 accounting for respectively 44% and 4% of the total abundance. However, in both cases a decrease of the abundance can be observed for this family during the phase 4, when the feeding was restarted and the ammonia concentration decreased.

The presence of microbes more specific of two subgroups of bioreactors (C1-Z3 and C2, C3, Z1 and Z2) was observed. In the first group (C1-Z3), members of the order Enterobacteriales were present at around 20-30% during all the experiment while these microbes never reached an abundance higher than 2% in the second group of bioreactors (C2 to Z2). Moreover, in the first group, a modification in the major OTU representative of this order was observed after ammonia addition. A decrease of an unknown genus of Enterobacteriaceae family was observed after day 70, beginning of the ammonia addition, followed a week after by the increase of the genus *Providencia*. The abundance of this genus decreased all along phase 3 (no feeding) to increase again at day 147. In the opposite, in the second group (C2 to Z2 bioreactors), the abundance of Burkholderiaceae family members increased from 1 to 8% since the addition of ammonia, while their abundances never exceeded 2% in the first group.

The microbial community, particularly the bacterial one, differed a bit between the bioreactors. If a core microbiome can be identified between all the bioreactors, subpopulations were found to be more specific between bioreactors C1 and Z3 on the one hand, and C2, C3, Z1 and Z2 on the other hand, showing that the presence of zeolite did not influence much the microbial composition in this experiment. While differences existed between the bioreactors, the modification in the microbial population from the ammonia inhibition to the recovery was in general similar and resulted in similar performances between all bioreactors.

Determination of the assembly processes shaping the community structure

In order to determine what was the part of deterministic and stochastic processes driving the microbial community assembly across the experiment, approaches based on phylogenetic diversity calculation and Neutral and null models tests were used.

The Nearest Taxon Index- (NTI) was used to compare the local community structure at each time points (figure 3-A). After the ammonia addition, a modification in the microbial structure was observed. The mean NTI taken across all communities was about 1.72 (p.value = $2.2e-16$) indicating phylogenetic clustering in average during the experiment. Indeed, the NTI value increased progressively during the phase 2 (ammonia inhibition) to progressively reach the value of 2 while standard deviation between the bioreactors decreased. This result indicates that the microbes with a short phylogenetic distance remained in all the bioreactors after the beginning of the

ammonia addition. After day 105 (Phase 3) the NTI value decreased slightly and the standard deviation increased, meaning that the coexistent taxons were less clustered, less phylogenetically close to each other, than in the previous phase, even if the NTI value did not reach the same level than during the stabilisation phase. The return of the feeding in the bioreactors did not seem to influence the microbial structuration after ammonia shock/inhibition. It could be hypothesized that microorganisms of the feeding (biowaste, kept at cold temperature, in aerobic conditions) were not able to provide additional microbial diversity in the digesters, which would probably induce an overdispersion in the phylogenetic distance (indicated by a $NTI < 2$), despite part of it was probably removed by the ammonia addition.

The percentage of stochasticity driving the microbial community assembly was determined by the Neutral model (figure 3-B), followed the same fluctuation than the NTI value. During the stabilisation phase the percentage of stochasticity decreased from 15% at day 49 to stabilise at around 12% at days 63 and 67. After the ammonia addition, the value decreased progressively to less than 9% until the middle of the Phase 3 (day 105). At day 118, the percentage increased to reach 12% and after few days, stabilised at 9%.

These results suggest that a drastic inhibition led to a more important clustering of the coexistent taxon close phylogenetically than during a stable period. This clustering was mainly shaped by deterministic processes. During this period, it was observed a sharp decrease of the performances and an increase of the VFA concentrations. The presence of ammonia induced a selection of the most resistant microbes, but not the most efficient regarding the methane production. After day 105, the microbial community assembly was less phylogenetically clustered and an increase in the stochastic processes seemed to indicate a part of a randomisation in the microbial adaptation facing ammonia. This period coincided with the return of the performances and a methane production through the hydrogenotrophic pathway.

Few studies determined the part of deterministic and stochastic processes in the microbial community structure during AD inhibition and recovery. In their study, Lin et al. (2017) observed that the microbial interactions were shaped by deterministic process in AD bioreactors operated at different temperature. Vanwongerghem et al., (2014) also observed that deterministic processes were involved in the AD microbial

community structuration. None of these studies focused on disturbance or recovery. However, in case of bioprocesses frequently subjected to disturbance, knowing if microbial community modification can be forecasted the possible prediction of the microbial community leading the bioprocess is important. Indeed, if stochastic processes drive the microbial structuration this would lead to different rearrangement of the microbial population with potentially different members during inhibition and/or after the recovery. This could modify the expected ecosystem function and lead to unpredictable performances.

Determination of the key microbes dynamics

The concentration of ammonia greatly influenced the dynamics of the microbial community in link with the bioreactors performances. OTUs driving the main source of variability were evidenced using sparse PCA. Based on the loading values of the OTUs in the PCA, 40 OTUs were selected. The corresponding taxonomic affiliation is reported (see supplementary materials). The sample plot obtained from the sPCA (figure 4), confirmed that the microbial community between the bioreactors followed a similar temporal dynamic. The modification in the microbial community started after the addition of ammonia at day 70 and stabilised when the feeding was stopped in the bioreactors (phase 3). Finally, the return of the feeding and the decrease of the ammonia concentration modified the microbial community. Once again, the result points out that the presence of zeolite was not the main source of variability in the microbial community.

The abundance of the selected microbes across the experiment is represented into a heatmap (figure 5). The microorganisms could be grouped in 5 clusters according to their dynamics across the different phases of the experiment.

Microbes sensitive to the presence of ammonia

Cluster 1 show the OTUs highly abundant at the beginning of the experiment. Their abundance decreased after the ammonia addition. This decrease was different between the microbes in this cluster probably due to a different sensitivity of the microbes facing ammonia. Four OTUs belonged to the phylum Bacteroidetes. Two syntrophic microbes were found in this cluster: *Smithella* (class Deltaproteobacteria) a butyrate and/or propionate syntrophic degrader, and *Syntrophorhabdus*, syntrophic microbe

living in association with archaea (Delforno et al., 2019). Zhang et al (2018) have shown previously that *Smithella* was moderately and severely inhibited at respectively 3 and 7-10 gNH₄⁺/L (Zhang et al., 2018). The genus *Acholeplasma* (class Mollicutes) was found also in this cluster. Divergent results regarding its sensitivity to the ammonia have been described. Indeed, in the study of Muller et al (2016), the abundance of *Acholeplasma* increased under increasing ammonia concentrations and was positively correlated to syntrophic-acetate oxidation pathway under ammonia inhibition (14 bioreactors including full-scale processes, 11gNH₄⁺/L maximum) (Müller et al., 2016). However, Fisher et al (2019) observed a decrease of the abundance of this microbe under increasing ammonia concentration (fed-batch bioreactors, 8g-TAN/L) (Fischer et al., 2019). In cluster 1, two OTUs belonging to the class Thermotogae, *Defluviitoga* and *Mesotoga* were found to be sensitive to the ammonia. These microbes are able to degrade carbohydrates and short-chain fatty acids into acetate and CO₂ and were mostly described in thermophilic bioreactors. *Defluviitoga* was shown to be tolerant to ammonia in high temperature (52°C) (Westerholm et al., 2018). In this study, its abundance decreased in regards to the increase of ammonia which implies sensitivity in mesophilic condition. Two OTUs from the archaea domain were influenced by the ammonia but in a different way. One OTU belonged to the *Methanosaeta* genus and its abundance decreased slowly compared to the other archaea *Methanoculleus* which was rapidly inhibited. As observed in the barplot figures, *Methanoculleus* was the main archaea in the system after the ammonia addition. At the beginning of the experiment, two OTUs belonging to the genus *Methanoculleus* were identified (OTUs 9 and 142). Just after the ammonia addition the OTU 9 took the lead and the OTU 142 disappeared. The OTU 9 was not selected by the sPCA probably because of its presence all along the experiment while the OTU 142 disappeared. In the same way, the absence of *Methanosarcina* in the selected OTU could be explained by its stable presence during all the experiment.

The decrease of microbes of cluster 1 can be associated to the presence of a high concentration of ammonia but also to the stop of the feeding, as most of the microbes are fermenters. However, no increase of their abundances was observed after the restart of the feeding. The microbes were inhibited by the presence of ammonia and could not overcome this inhibition, or their ecological niches were not free anymore

and they could not grow again. Further studies on their functional activity should be carried out to answer this question.

Specific microbes tolerant to the presence of ammonia

In the cluster 2 are highlighted two OTUs which seemed to be tolerant to the ammonia as their abundances did not decrease specifically after ammonia addition. However, these OTUs were present only in some bioreactors, mostly C3 and Z1. They belong to the unknown Rikenellaceae DMER64 and *Providencia* genus (Enterobacteriaceae family). Rikenellaceae DMER64 is a VFAs, CO₂, NH₃ and H₂ producer and a negative effect of high abundance of H₂ on its development was observed (Wahid et al., 2019). *Providencia* genus is known to have a high cellulolytic activity and plays an important role during the hydrolysis step. The presence of these two fermenters in only two over the six bioreactors did not lead to modification in the performances nor the dynamics of the population in these bioreactors.

Microbes tolerant to the presence of ammonia

The abundance of the microbes from cluster 3 were relatively abundant at the beginning of the experiment but decreased when ammonia was added into the bioreactors. Their abundance finally increased again when the level of ammonia was below 1.5 gTAN/L (after day 147). This cluster contains 9 OTUs mostly represented by the Firmicutes and Bacteroidetes phyla. These two orders are mostly proteolytic microbes and fermenters. From the Bacteroidetes phyla, the genus *Proteiniphilum* is an amino-acid degrader which produces VFAs such as acetate and propionate. One *Petrimonas* genus was found in this cluster. However, another member of this genus was found in the cluster 1 (sensitive to ammonia) was also found. Species from this genus seemed to be differently affected by the ammonia. In a previous study, a bimodal response was observed for *Petrimonas* (class Bacteroidia) with a decrease of their abundance at 5 gTAN/L and an increase at 8 gTAN/L (Zeb et al., 2019).

From the Firmicutes phyla, genera *Hydrogenispora*, *Proteiniclasticum*, *Cellulosilyticum* and *Ruminococcaceae* were detected in this cluster. *Proteiniclasticum* was determined to be sensitive but able to maintain in increased concentration of ammonia. *Cellulosilyticum* is a lignocellulosic degrader. *Hydrogenispora* can produce H₂, ethanol, and acetate by fermentation of various

saccharides. This microbe was found to be able to maintain under increasing ammonia condition and is suspected to be able of syntrophic interaction with the hydrogenotrophic archaea (Kougias et al., 2017). This would be relevant in this study as the methane was mainly produced through the hydrogenotrophic pathway during the inhibition phases. *Advenella* genus (class Gammaproteobacteria) was also found in this cluster.

Clusters 1 and 3 grouped together microbes present at the beginning of the experiment but presenting a sensitivity to a concentration of ammonia higher than 4 gTAN/L. However, microbes in cluster 3 seemed to be more resistant than the ones in cluster 1 as their abundances increased again when the concentration of ammonia decreased at the end of the experiment.

Microbes favoured by the presence of ammonia

In the clusters 4 and 5 the microbes favoured by the presence of ammonia are highlighted. These microbes were absent or with very low abundances during the stabilisation phase but developed after the addition of ammonia. The differences between these two clusters come from 1) the moment when the abundances of these microbes started to increase. Indeed, cluster 4 grouped together the microbes that developed just after the ammonia addition, while microbes from the cluster 5 appeared a week after; and 2) the abundances of the microbes increased until the end of the experiment, even when the ammonia concentration was low while it was not the case for microbes in cluster 4. In these two clusters, microbes from the phylum Firmicutes and 1 OTU from the phylum Tenericutes were found.

In cluster 4, OTUs belonging to the genus *Bacillus* were found. Their ability to produce high amount of H₂ from the hydrolysis of organic compounds has been demonstrated previously (Meier et al., 2020). Yu et al (2014) applied a bioaugmentation using *Bacillus cereus*, identified as ammonia-resistant organism, to treat landfill leachate (Yu et al., 2014). These results suggest a beneficial role of the ammonia on the development of this microbe, potentially linked to the development of hydrogenotrophic archaea such as *Methanoculleus*. The potential role of *Bacillus* in the methane production through an interaction with hydrogenotrophic archaea, ie as possible syntrophic-acetate oxidizer, should be further investigated. *Natronincola* genus is an alkaline microbe able to ferment peptides and seemed to be able to grow

under high H₂ partial pressure as it was found to be abundant during a biomethanation process (Braga Nan et al., 2020). *Syntrophomonas* is a butyric-acid degrader in syntrophy with methanogens. *Syntrophomonas* was already described as an ammonia-resistant microbe in a previous study (Bonk et al., 2018) which is in line with the result presented in this present article. *Defluviitalea* (clusters 4 and 5) and *Tepidimicrobium* (cluster 5) were previously found in different studies as ammonia-resistant microbes. In their study, Poirier et al (2020) identified these two microbes as potential bioindicators of ammonia inhibition by comparing several studies (Poirier et al., 2020).

In addition in cluster 5, were found *Desulfuribacillus*, involved in sulfidogenesis in anaerobic conditions (Sorokin et al., 2012). MBA03 clade from Clostridia class was determined as part of core microbiome in mesophilic and thermophilic AD process. This microbe was evidenced to be an electroactive genus and a potential partner of *Methanosarcina* in the syntrophic acetate oxidation (Calusinska et al., 2018). *Izimaplasmatales* order was previously found in bioreactor only containing zeolite and 4 gTAN/L of ammonia (Cardona et al., 2020). In the current study, it can be observed that the abundance *Izimaplasmatales* increased mainly at the end of the experiment when ammonia concentration decreased to reach 2 gTAN/L. On the contrary than the study from Cardona et al (2020), *Izimaplasmatales* was found in all the bioreactors, with or without zeolite. The role of this microbe in the bioreactor is still unclear and would need further investigation.

In both these clusters mostly microbes involved or potentially involved in syntrophy with hydrogenotrophic archaea were found. Their development from the ammonia inhibition phase makes sense with the development of *Methanoculleus* and the methane production through hydrogenotrophic pathway evidenced by the biogas isotopic fractionation analysis. This also suggests the possibility of the syntrophic acetate oxidation to take place into the bioreactors to produce methane. Microbes from cluster 5 were highly abundant during the last period of the experiment, especially *Izimaplasmatales*, MBA03 and *Desulfuribacillus*. This could be explained or by the higher availability of these microbes to face the development of the microbes from the cluster 3 and maintain into their niche and/or a low dependency to the syntrophy when this one is less required in low stress condition.

The influence of the starvation must also be taken into account in the microbial dynamics. Feeding was interrupted during phase 3 as the biogas production stopped after the addition of ammonia. Short and long term starvation in anaerobic digester has been studied and can cause a reduction in the methane production and a modification in the microbial population composition at the restart period (Hwang et al., 2010). Regarding the methanogens it has been observed a longer lag phase than for acidogens, probably due to their lower growth rate. In this study, it was observed a slightly lower biogas production after the starvation and the return of feeding than during the stabilisation phase. This could be explained by modifications in the microbial population especially regarding relative abundance of the different members. The dynamics of the different members of the microbial population could be explained by the addition of ammonia coupled to the starvation phase. Microbes from clusters 1 and 3 were hardly impacted and their abundances decreased for the benefit of microbes from the clusters 4 and 5. After the starvation phase and during the return of the feeding microbes from cluster 1 were probably not able to compete anymore with the microbes from clusters 2 and 5 for which the abundances were still higher than for the clusters 1 and 4. It is difficult to distinguish the influence of the starvation to the ammonia addition. Moreover, this result highlights the limitation of using 16S rRNA coding gene sequencing instead of 16S rRNA sequencing. Indeed, in the case of DNA all microbes, even those in dormancy or dead, are detected instead of just the one active in the case of the RNA.

The use of local α -diversity (represented by the NTI) and the null-model allowed to determine that under high inhibition the microbial diversity decreased and the structuration of the different members was driven by deterministic processes. This result is in line with the classical concept regarding the relationship between diversity and disturbance. Under extreme conditions, the diversity decreases due to a selection of the most adaptive members of the community. This is mainly driven by deterministic mechanisms. Under intermediate disturbance, specialised traits are less advantageous for the microbes due to unpredictable environment and this result in higher diversity (Santillan et al., 2019) shaped by stochastic mechanisms. In this study, only strong inhibition was tested. Further studies should be designed to evaluate the part of stochastic-deterministic mechanisms under different type of disturbances, press versus pulse disturbance, and low to high level of disturbance in

order to determine the predictability of the microbial structuration to further be able to better manage the AD bioprocess.

Conclusion

The dynamics of the microbial community was comparable between six bioreactors even after a drastic failure on the bioprocess, indicating a deterministic process for the recovery. Despite the presence of different subpopulations between the bioreactors, no complete restructuration of the microbial community was observed. It raises the question of the role of these microbes in the overall microbial community activity. If the hydrogenotrophic methanogenesis was the main pathway for methane production in presence of ammonia, both methane production pathways were observed after the recovery. Further studies regarding the the potential functional redundancy of the microbiome should be performed.

E-supplementary material

E-supplementary data for this work can be found in e-version of this paper online.

Acknowledgements

Great thank goes to Angeline Guenne, Nadine Derlet and Chrystelle Bureau from the analytical division from INRAE PROSE for their technical support.

Funding

This work was supported by the National Research Agency (ANR-16-CE05-0014).

References

Akindede, A.A., Sartaj, M., 2018. The toxicity effects of ammonia on anaerobic digestion of organic fraction of municipal solid waste. *Waste Manag.* 71, 757–766. <https://doi.org/10.1016/j.wasman.2017.07.026>

Anthonisen, A., Loehr, R., Prakasam, T., Srinath, E., 1976. Inhibition of Nitrification by Ammonia and Nitrous Acid. *J. Water Pollut. Control Fed.* 48, 835–852. <https://doi.org/10.1017/CBO9781107415324.004>

Bonk, F., Popp, D., Weinrich, S., Sträuber, H., Kleinsteuber, S., Harms, H., Centler, F., 2018. Ammonia Inhibition of Anaerobic Volatile Fatty Acid Degrading Microbial Communities. *Front. Microbiol.* 9, 1–13. <https://doi.org/10.3389/fmicb.2018.02921>

Braga Nan, L., Trably, E., Santa-Catalina, G., Bernet, N., Delgenès, J.-P., Escudié, R., 2020. Biomethanation processes: new insights on the effect of a high H₂ partial pressure on microbial communities. *Biotechnol. Biofuels* 13, 141. <https://doi.org/10.1186/s13068-020-01776-y>

Calusinska, M., Goux, X., Fossépré, M., Muller, E.E.L., Wilmes, P., Delfosse, P., 2018. A year of monitoring 20 mesophilic full-scale bioreactors reveals the existence of stable but different core microbiomes in bio-waste and wastewater anaerobic digestion systems. *Biotechnol. Biofuels* 11, 196. <https://doi.org/10.1186/s13068-018-1195-8>

Cardona, L., Mazéas, L., Chapleur, O., 2020. Zeolite favours propionate syntrophic degradation during anaerobic digestion of food waste under low ammonia stress. *Chemosphere* 594, 127932. <https://doi.org/10.1016/j.chemosphere.2020.127932>

Chase, J.M., Myers, J.A., 2011. Disentangling the importance of ecological niches from stochastic processes across scales. *Philos. Trans. R. Soc. B Biol. Sci.* 366, 2351–2363. <https://doi.org/10.1098/rstb.2011.0063>

Chen, Y., Cheng, J.J., Creamer, K.S., 2008. Inhibition of anaerobic digestion process: A review. *Bioresour. Technol.* 99, 4044–4064. <https://doi.org/10.1016/j.biortech.2007.01.057>

Delforno, T.P., Macedo, T.Z., Midoux, C., Lacerda, G. V., Rué, O., Mariadassou, M., Loux, V., Varesche, M.B.A., Bouchez, T., Bize, A., Oliveira, V.M., 2019. Comparative metatranscriptomic analysis of anaerobic digesters treating anionic surfactant contaminated wastewater. *Sci. Total Environ.* 649, 482–494. <https://doi.org/10.1016/j.scitotenv.2018.08.328>

Escudié, F., Auer, L., Bernard, M., Mariadassou, M., Cauquil, L., Vidal, K., Maman, S., Hernandez-Raquet, G., Combes, S., Pascal, G., 2018. FROGS: Find, Rapidly, OTUs with Galaxy Solution. *Bioinformatics* 34, 1287–1294.

- Fernández, N., Montalvo, S., Fernández-Polanco, F., Guerrero, L., Cortés, I., Borja, R., Sánchez, E., Travieso, L., 2007. Real evidence about zeolite as microorganisms immobilizer in anaerobic fluidized bed reactors. *Process Biochem.* 42, 721–728. <https://doi.org/10.1016/j.procbio.2006.12.004>
- Fischer, M.A., Ulbricht, A., Neuling, S.C., Refai, S., Waßmann, K., Künzel, S., Schmitz, R.A., 2019. Immediate Effects of Ammonia Shock on Transcription and Composition of a Biogas Reactor Microbiome. *Front. Microbiol.* 10. <https://doi.org/10.3389/fmicb.2019.02064>
- Fotidis, I.A., Kougias, P.G., Zaganas, I.D., Kotsopoulos, T.A., Martzopoulos, G.G., 2014. Inoculum and zeolite synergistic effect on anaerobic digestion of poultry manure. *Environ. Technol. (United Kingdom)* 35, 1219–1225. <https://doi.org/10.1080/09593330.2013.865083>
- Hwang, K., Song, M., Kim, W., Kim, N., Hwang, S., 2010. Effects of prolonged starvation on methanogenic population dynamics in anaerobic digestion of swine wastewater. *Bioresour. Technol.* 101, S2–S6. <https://doi.org/10.1016/j.biortech.2009.03.070>
- Jiang, Y., McAdam, E., Zhang, Y., Heaven, S., Banks, C., Longhurst, P., 2019. Ammonia inhibition and toxicity in anaerobic digestion: A critical review. *J. Water Process Eng.* 32, 100899. <https://doi.org/10.1016/j.jwpe.2019.100899>
- Kembel, S.W., Cowan, P.D., Helmus, M.R., Cornwell, W.K., Morlon, H., Ackerly, D.D., Blomberg, S.P., Webb, C.O., 2010. Picante: R tools for integrating phylogenies and ecology. *Bioinformatics* 26, 1463–1464. <https://doi.org/10.1093/bioinformatics/btq166>
- Kougias, P.G., Treu, L., Benavente, D.P., Boe, K., Campanaro, S., Angelidaki, I., 2017. Ex-situ biogas upgrading and enhancement in different reactor systems. *Bioresour. Technol.* 225, 429–437. <https://doi.org/10.1016/j.biortech.2016.11.124>
- Lin, Q., De Vrieze, J., Li, C., Li, Jiaying, Li, Jiabao, Yao, M., Hedenec, P., Li, H., Li, T., Rui, J., Frouz, J., Li, X., 2017. Temperature regulates deterministic processes and the succession of microbial interactions in anaerobic digestion process. *Water Res.* 123, 134–143. <https://doi.org/10.1016/j.watres.2017.06.051>

- Mawson, A.J., Earle, R.L., Larsen, V.F., 1991. Degradation of acetic and propionic acids in the methane fermentation. *Water Res.* 25, 1549–1554. [https://doi.org/10.1016/0043-1354\(91\)90187-U](https://doi.org/10.1016/0043-1354(91)90187-U)
- McMurdie, P.J., Holmes, S., 2013. Phyloseq: An R Package for Reproducible Interactive Analysis and Graphics of Microbiome Census Data. *PLoS One* 8. <https://doi.org/10.1371/journal.pone.0061217>
- Meier, T.R.W., Cremonez, P.A., Maniglia, T.C., Sampaio, S.C., Teleken, J.G., da Silva, E.A., 2020. Production of biohydrogen by an anaerobic digestion process using the residual glycerol from biodiesel production as additive to cassava wastewater. *J. Clean. Prod.* 258, 120833. <https://doi.org/10.1016/j.jclepro.2020.120833>
- Milán, Z., Sánchez, E., Weiland, P., Borja, R., Martín, A., Ilangovan, K., 2001. Influence of different natural zeolite concentrations on the anaerobic digestion of piggery waste. *Bioresour. Technol.* 80, 37–43. [https://doi.org/10.1016/S0960-8524\(01\)00064-5](https://doi.org/10.1016/S0960-8524(01)00064-5)
- Montalvo, S., Díaz, F., Guerrero, L., Sánchez, E., Borja, R., 2005. Effect of particle size and doses of zeolite addition on anaerobic digestion processes of synthetic and piggery wastes. *Process Biochem.* 40, 1475–1481. <https://doi.org/10.1016/j.procbio.2004.06.032>
- Mosbæk, F., Kjeldal, H., Mulat, D.G., Albertsen, M., Ward, A.J., Feilberg, A., Nielsen, J.L., 2016. Identification of syntrophic acetate-oxidizing bacteria in anaerobic digesters by combined protein-based stable isotope probing and metagenomics. *ISME J.* 10, 2405–2418. <https://doi.org/10.1038/ismej.2016.39>
- Müller, B., Sun, L., Westerholm, M., Schnürer, A., 2016. Bacterial community composition and fhs profiles of low- and high-ammonia biogas digesters reveal novel syntrophic acetate-oxidising bacteria. *Biotechnol. Biofuels* 9, 1–18. <https://doi.org/10.1186/s13068-016-0454-9>
- Peces, M., Astals, S., Jensen, P.D., Clarke, W.P., 2018. Deterministic mechanisms define the long-term anaerobic digestion microbiome and its functionality regardless of the initial microbial community. *Water Res.* 141, 366–376. <https://doi.org/10.1016/j.watres.2018.05.028>

Poirier, S., Déjean, S., Midoux, C., Lê Cao, K.-A., Chapleur, O., 2020. Integrating independent microbial studies to build predictive models of anaerobic digestion inhibition by ammonia and phenol. *Bioresour. Technol.* 316, 123952. <https://doi.org/10.1016/j.biortech.2020.123952>

Poirier, S., Madigou, C., Bouchez, T., Chapleur, O., 2017. Improving anaerobic digestion with support media: Mitigation of ammonia inhibition and effect on microbial communities. *Bioresour. Technol.* 235, 229–239. <https://doi.org/10.1016/j.biortech.2017.03.099>

Rohart, F., Gautier, B., Singh, A., Lê Cao, K.-A., 2017. mixOmics: An R package for ‘omics feature selection and multiple data integration. *PLOS Comput. Biol.* 13, e1005752. <https://doi.org/10.1371/journal.pcbi.1005752>

Ruiz-Sánchez, J., Guivernau, M., Fernández, B., Vila, J., Viñas, M., Riau, V., Prenafeta-Boldú, F.X., 2019. Functional biodiversity and plasticity of methanogenic biomass from a full-scale mesophilic anaerobic digester treating nitrogen-rich agricultural wastes. *Sci. Total Environ.* 649, 760–769. <https://doi.org/10.1016/j.scitotenv.2018.08.165>

Santillan, E., Seshan, H., Constancias, F., Drautz-Moses, D.I., Wuertz, S., 2019. Frequency of disturbance alters diversity, function, and underlying assembly mechanisms of complex bacterial communities. *npj Biofilms Microbiomes* 5, 8. <https://doi.org/10.1038/s41522-019-0079-4>

Shen, H., Huang, J.Z., 2008. Sparse principal component analysis via regularized low rank matrix approximation. *J. Multivar. Anal.* 99, 1015–1034. <https://doi.org/10.1016/j.jmva.2007.06.007>

Sloan, W.T., Lunn, M., Woodcock, S., Head, I.M., Nee, S., Curtis, T.P., 2006. Quantifying the roles of immigration and chance in shaping prokaryote community structure. *Environ. Microbiol.* 8, 732–740. <https://doi.org/10.1111/j.1462-2920.2005.00956.x>

Sorokin, D.Y., Tourova, T.P., Sukhacheva, M. V., Muyzer, G., 2012. *Desulfuribacillus alkaliarsenatis* gen. nov. sp. nov., a deep-lineage, obligately anaerobic, dissimilatory sulfur and arsenate-reducing, haloalkaliphilic representative

of the order Bacillales from soda lakes. *Extremophiles* 16, 597–605. <https://doi.org/10.1007/s00792-012-0459-7>

Stegen, J.C., Lin, X., Konopka, A.E., Fredrickson, J.K., 2012. Stochastic and deterministic assembly processes in subsurface microbial communities. *ISME J.* 6, 1653–1664. <https://doi.org/10.1038/ismej.2012.22>

Treu, L., Kougias, P.G., Campanaro, S., Bassani, I., Angelidaki, I., 2016. Deeper insight into the structure of the anaerobic digestion microbial community; the biogas microbiome database is expanded with 157 new genomes. *Bioresour. Technol.* 216, 260–266. <https://doi.org/10.1016/j.biortech.2016.05.081>

Vanwonterghem, I., Jensen, P.D., Dennis, P.G., Hugenholtz, P., Rabaey, K., Tyson, G.W., 2014. Deterministic processes guide long-term synchronised population dynamics in replicate anaerobic digesters. *ISME J.* 8, 2015–2028. <https://doi.org/10.1038/ismej.2014.50>

Wahid, R., Mulat, D.G., Gaby, J.C., Horn, S.J., 2019. Effects of H₂:CO₂ ratio and H₂ supply fluctuation on methane content and microbial community composition during in-situ biological biogas upgrading. *Biotechnol. Biofuels* 12, 104. <https://doi.org/10.1186/s13068-019-1443-6>

Wang, H., Fotidis, I.A., Angelidaki, I., 2015. Ammonia effect on hydrogenotrophic methanogens and syntrophic acetate-oxidizing bacteria. *FEMS Microbiol. Ecol.* 91, 1–8. <https://doi.org/10.1093/femsec/fiv130>

Wang, Q., Garrity, G.M., Tiedje, J.M., Cole, J.R., 2007. Naive Bayesian classifier for rapid assignment of rRNA sequences into the new bacterial taxonomy. *Appl. Environ. Microbiol.* 73, 5261–7. <https://doi.org/10.1128/AEM.00062-07>

Wang, Q., Yang, Y., Yu, C., Huang, H., Kim, M., Feng, C., Zhang, Z., 2011. Study on a fixed zeolite bioreactor for anaerobic digestion of ammonium-rich swine wastes. *Bioresour. Technol.* 102, 7064–7068. <https://doi.org/10.1016/j.biortech.2011.04.085>

Wang, Y., Qian, P.Y., 2009. Conservative fragments in bacterial 16S rRNA genes and primer design for 16S ribosomal DNA amplicons in metagenomic studies. *PLoS One* 4. <https://doi.org/10.1371/journal.pone.0007401>

Webb, C.O., Ackerly, D.D., McPeck, M.A., Donoghue, M.J., 2002. Phylogenies and Community Ecology. *Annu. Rev. Ecol. Syst.* 33, 475–505. <https://doi.org/10.1146/annurev.ecolsys.33.010802.150448>

Westerholm, M., Isaksson, S., Karlsson Lindsjö, O., Schnürer, A., 2018. Microbial community adaptability to altered temperature conditions determines the potential for process optimisation in biogas production. *Appl. Energy* 226, 838–848. <https://doi.org/10.1016/j.apenergy.2018.06.045>

Whiticar, M.J., Faber, E., Schoell, M., 1986. Biogenic methane formation in marine and freshwater environments: CO₂reduction vs. acetate fermentation-Isotope evidence. *Geochim. Cosmochim. Acta* 50, 693–709. [https://doi.org/10.1016/0016-7037\(86\)90346-7](https://doi.org/10.1016/0016-7037(86)90346-7)

Yu, D., Yang, J., Teng, F., Feng, L., Fang, X., Ren, H., 2014. Bioaugmentation Treatment of Mature Landfill Leachate by New Isolated Ammonia Nitrogen and Humic Acid Resistant Microorganism. *J. Microbiol. Biotechnol.* 24, 987–997. <https://doi.org/10.4014/jmb.1401.01066>

Yuan, H., Mei, R., Liao, J., Liu, W.-T., 2019. Nexus of Stochastic and Deterministic Processes on Microbial Community Assembly in Biological Systems. *Front. Microbiol.* 10, 1–12. <https://doi.org/10.3389/fmicb.2019.01536>

Zeb, I., Ma, J., Mehboob, F., Kafle, G.K., Amin, B.A.Z., Nazir, R., Ndegwa, P., Frear, C., 2019. Kinetic and microbial analysis of methane production from dairy wastewater anaerobic digester under ammonia and salinity stresses. *J. Clean. Prod.* 219, 797–808. <https://doi.org/10.1016/j.jclepro.2019.01.295>

Zhang, C., Yuan, Q., Lu, Y., 2018. Inhibitory effects of ammonia on syntrophic propionate oxidation in anaerobic digester sludge. *Water Res.* 146, 275–287. <https://doi.org/10.1016/j.watres.2018.09.046>

Zhou, J., Deng, Y., Zhang, P., Xue, K., Liang, Y., Van Nostrand, J.D., Yang, Y., He, Z., Wu, L., Stahl, D.A., Hazen, T.C., Tiedje, J.M., Arkin, A.P., 2014. Stochasticity, succession, and environmental perturbations in a fluidic ecosystem. *Proc. Natl. Acad. Sci.* 111, E836–E845. <https://doi.org/10.1073/pnas.1324044111>

Figure captions

Figure 1. Schematic representation of the experimental design. Phase 1 corresponds to the stabilisation phase; Phase 2 to the ammonia shock; Phase 3 to the stop of the feeding; Phase 4 to the restart of the feeding

Figure 2. Evolution of the chemical parameters. Red line represents the beginning of Phase 2 (ammonia addition). Blue line represents the beginning of Phase 3 (stop feeding) and purple line represents the beginning of the Phase 4 (feeding restart). Dashed lines represent the sampling points for the 16S rRNA gene amplicon sequencing

Figure 3: Microbial community assembly. A) Nearest taxon index (NTI) values for each time points estimated using the 6 bioreactors. $NTI > +2$ (or < -2) indicates coexisting taxa are more (or less) closely related than expected by chance. Red line represents the beginning of Phase 2 (ammonia addition). Blue line represents the beginning of Phase 3 (stop feeding) and violet line represents the beginning of the Phase 4 (feeding restart). B) Percentage of stochasticity determining using null model. Mean values and error bars were obtained from the simulated results obtained for each replicate.

Figure 4. Microbial dynamics over time with respect to the presence of zeolite. Sample plot from the sPCA from the 16S rRNA amplicon sequencing dataset. Bioreactors series C (without zeolite) and Z (with zeolite) are represented by different symbols and samples taken at the same day are grouped with stars.

Figure 5. Heatmap of the microorganisms whose abundance contributes the most to the variance due to temporal dynamics, selected with sPCA. Taxonomy is indicated at the genus level when available, otherwise order level is given. Abundance is represented in the heatmap with colors ranging from blue (low) to high (red). Stars indicate archaea.

Figures

Figure 1

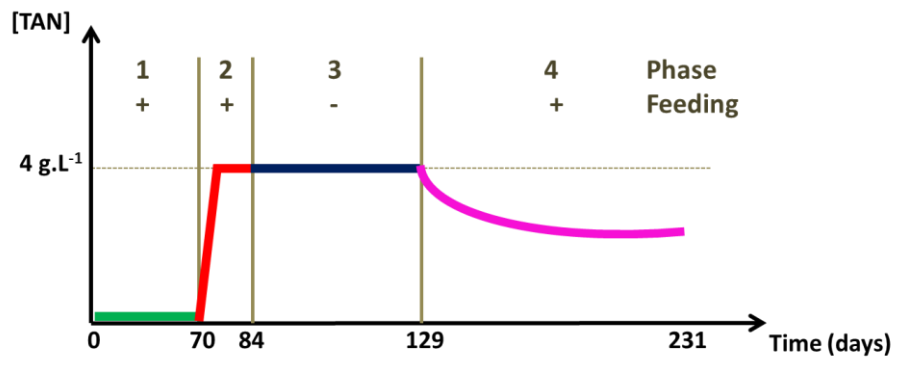


Figure 2

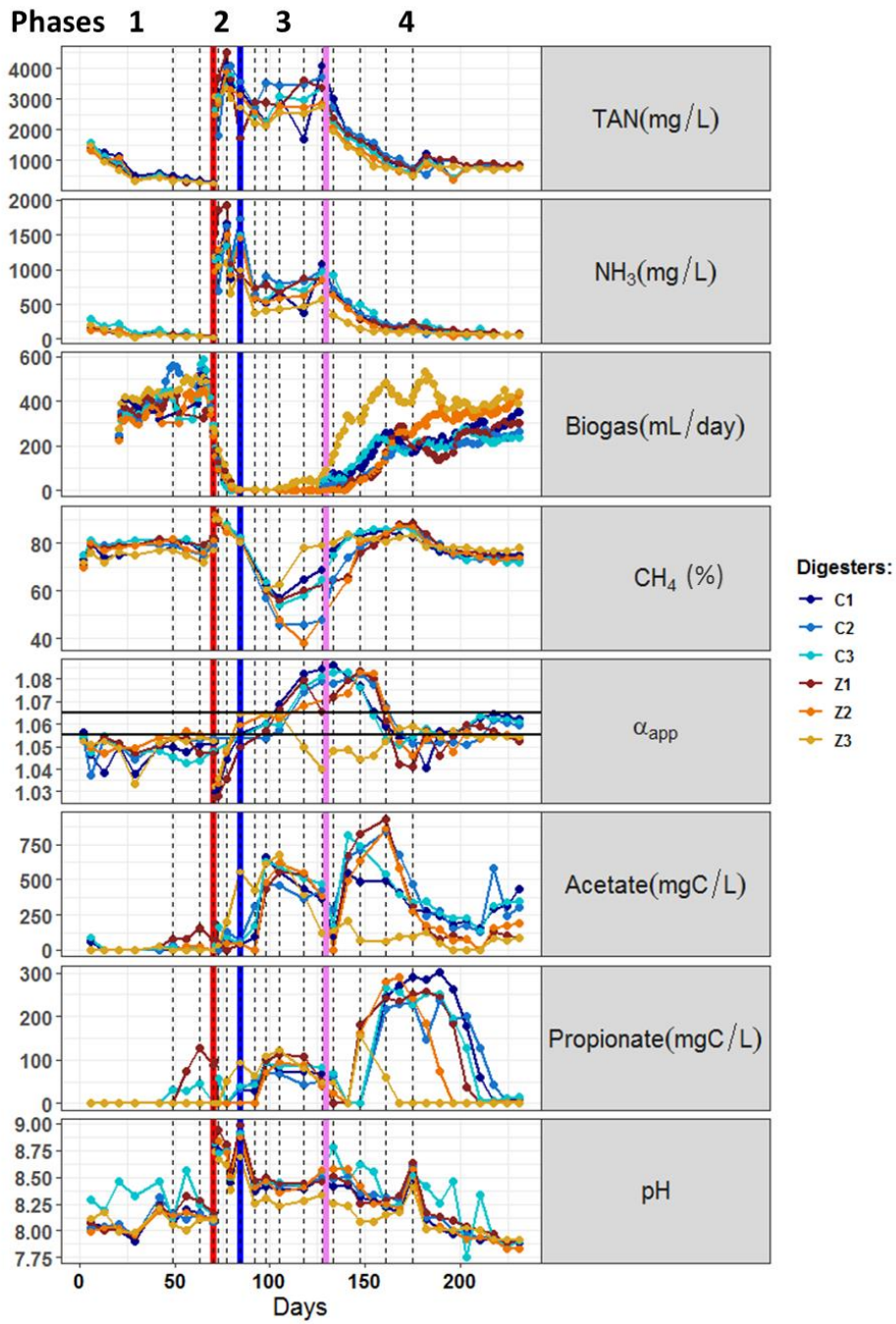


Figure 3

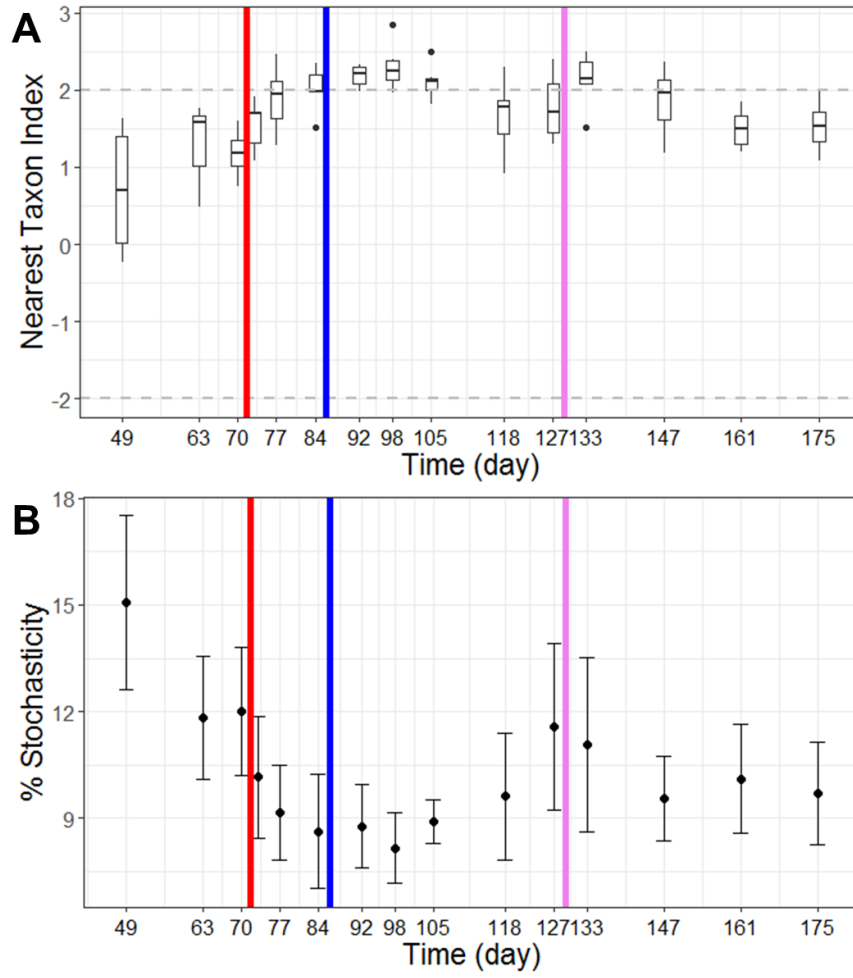


Figure 4

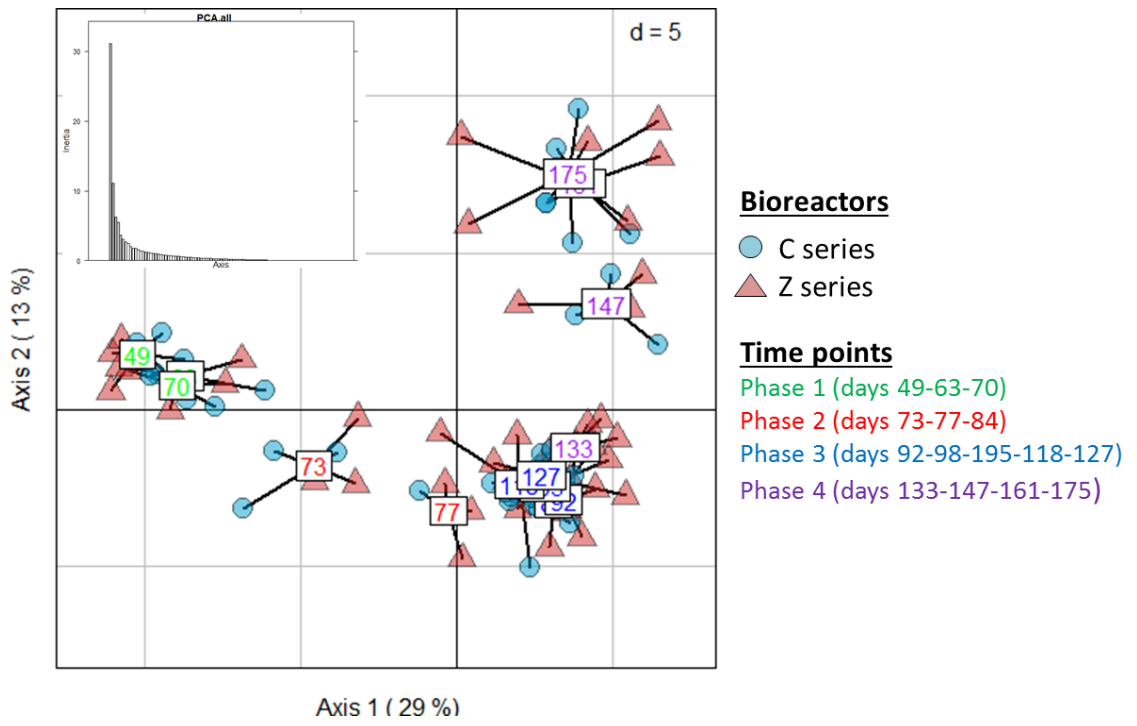


Figure 5

